

Solitary Pulse Generation by Backward Raman Scattering in H₂-Filled Photonic Crystal Fibers

A. Abdolvand,^{1,*} A. Nazarkin,^{1,*} A. V. Chugreev,^{1,*} C. F. Kaminski,^{2,3,†} and P. St.J. Russell^{1,*}

¹Max-Planck Institute for the Science of Light, Guenther-Scharowsky Str. 1/24, D-91058 Erlangen, Germany

²Department of Chemical Engineering and Biotechnology, University of Cambridge, CB2 3RA, United Kingdom

³SAOT, University of Erlangen-Nuremberg, Erlangen, Germany

(Received 28 July 2009; revised manuscript received 30 September 2009; published 29 October 2009)

Using a hydrogen-filled hollow-core photonic crystal fiber as a nonlinear optical gas cell, we study amplification of ns-laser pulses by backward rotational Raman scattering. We find that the amplification process has two characteristic stages. Initially, the pulse energy grows and its duration shortens due to gain saturation at the trailing edge of the pulse. This phase is followed by formation of a symmetric pulse with a duration significantly shorter than the phase relaxation time of the Raman transition. Stabilization of the Stokes pulse profile to a solitonlike hyperbolic secant shape occurs as a result of nonlinear amplification at its front edge and nonlinear absorption at its trailing edge (caused by energy conversion back to the pump field), leading to a reshaped pulse envelope that travels at superluminal velocity.

DOI: 10.1103/PhysRevLett.103.183902

PACS numbers: 42.70.Qs, 42.50.Md, 42.65.Dr, 42.65.Ky

Stimulated Raman scattering of light (SRS) exhibits remarkably diverse behavior in different regimes and interaction conditions, and is the continuing subject of research. When SRS occurs in a counterpropagating geometry (backward stimulated Raman scattering or BSRS), the Raman process exhibits particularly interesting spatiotemporal dynamics [1,2]. In contrast to forward SRS where pump and Raman signal copropagate, in BSRS the signal can extract energy stored throughout the whole amplifying region. As a result, the Stokes pulse can reach a peak power far in excess of the pump power. Moreover, due to depletion of the pump wave from the leading to the trailing edge of the Stokes pulse, the Raman gain saturates, leading to a strong steepening and sharpening of the Stokes pulse, a mechanism that has found important applications in high energy, short pulse laser physics [3].

In early BSRS experiments it was observed that the generated Stokes pulses could have durations on the order of T_2 , the phase relaxation time of the molecular vibrations (or rotations) [2]. This raises the interesting question of whether nonlinear pulse shortening is possible in the highly transient regime [4,5], where the pulse duration is much shorter than T_2 . Assuming Stokes pulse amplification by an infinitely long counterpropagating pump wave one can find, from the exact equations of BSRS [2], that in the presence of linear loss the asymptotic solution is a steady-state pulse:

$$I_s(z, t) \propto \text{sech}^2\left(\frac{t - z/v_s}{\tau_s}\right) \quad (1)$$

moving with the velocity of light v_s and having a duration $\tau_s = T_2 \gamma_s / G_s$, where γ_s is the linear loss coefficient and G_s is the steady-state Raman gain. According to Eq. (1), for a sufficiently high Raman gain (or low loss), so that the condition $\gamma_s / G_s \ll 1$ is fulfilled, the Stokes pulse duration can be much shorter than T_2 . This might suggest that, intrinsically, the mechanism of pulse shortening by BSRS

is not limited by the buildup time of the molecular response of the Raman medium. So far, a detailed experimental study of transient effects in SRS has been difficult. In a focused beam geometry, the interaction length is limited by beam diffraction, and to observe SRS at a sub- T_2 time scale one needs to pump at multi-gigawatt powers, which leads to beam self-focusing, self-phase modulation and the generation of additional SRS components [5–7].

Here we make use of the unique characteristics of gas-filled hollow-core photonic crystal fiber (HC-PCF) [8] in a detailed study of BSRS. By eliminating beam diffraction, these novel optical guiding systems offer interaction lengths many times longer than the Rayleigh length of a focused laser beam, while keeping the laser beam tightly confined in a single mode. As a result, the threshold power for SRS can be dramatically reduced [9] below the threshold for deleterious competing nonlinear effects. Moreover, using HC-PCF with a specially engineered guidance band, the Raman process can be isolated from competing SRS processes [10]. By means of this approach, we are able to gain deeper insight into the different stages of Stokes amplification by BSRS. We demonstrate pulse amplification and shortening below T_2 . Well before the pulse reaches its asymptotic shape (1), the amplification saturates due to formation of a reshaped pulse envelope propagating at a superluminal velocity. This reshaping occurs as a result of the combined action of nonlinear amplification at the pulse leading edge and nonlinear absorption at its trailing edge—an effect similar to 2π -pulse dynamics in laser amplifiers [11]. The results represent a significant advance in the study of coherent effects [4,5,12], and point to a new generation of highly engineerable optical gas cells for studying complex nonlinear phenomena.

The Fig. 1 shows the setup used, comprising a narrow linewidth pump laser emitting 50 μ J pulses of 12 ns duration at 1.064 μ m. The seed Stokes pulses were generated by forward SRS in a 1.5 m long band gap guiding HC-PCF

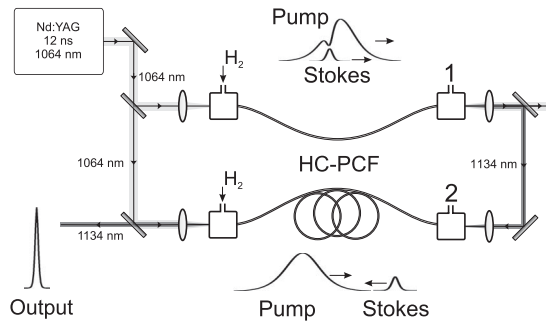


FIG. 1. Schematic of the experimental setup for the study of pulse amplification by backward rotational SRS in a hydrogen-filled HC-PCF.

filled with hydrogen (stage I). The BRS process was studied in a second stage, consisting of an additional length of hydrogen-filled fiber. The Raman-active transition between the levels $J = 1$ and $J = 3$ of molecular hydrogen (Raman shift = 587 cm^{-1} [13]) was chosen to study transient BRS. The transmission window of the HC-PCF was designed to feature low loss transmission only for the pump and the first Stokes frequencies. This means that the BRS process was completely decoupled from the competing vibrational and higher order rotational SRS processes which are typically present in a focused beam geometry. The BRS gain profile of hydrogen exhibits both Doppler and collisional broadening [14]. The line broadening due to molecular collisions (MC) is pressure dependent (for H_2 the broadening is $\Delta\nu_{\text{MC}} = 50 \text{ MHz/bar}$), so that to observe coherent effects with a few ns pulse one should operate at relatively low pressures ($< 3 \text{ bar}$). In this regime, the phase relaxation is mainly due to collisions with the sidewalls (corresponding linewidth $\Delta\nu_{\text{wall coll.}} = 200 \text{ MHz}$), resulting in an effective phase relaxation time at 3 bar of $T_2 = 3.5 \text{ ns}$. In this pressure regime, the energy relaxation time is significantly longer ($T_1 > 15 \text{ ns}$) [15]. The pump intensity and gas pressure in the first fiber were optimized so that the steepness of the leading edge of the generated Stokes pulse was maximized (the importance of this adjustment is discussed below). The energy of the output pulse was $\approx 4 \mu\text{J}$ with a duration of 7 ns (approximately twice the value of T_2 in the subsequent amplification stage). The length and the pressure in the second fiber were chosen to maximize the gain factor for the seed pulse while ensuring that the pump pulse energy remained below the threshold for forward SRS.

Figure 2 shows the evolution of the temporal structure of the BRS Stokes pulse for increasing pump pulse energies at a pressure of 3 bar. Amplification of the Stokes field occurs predominantly at the leading edge of the pulse, giving rise to formation of an intense spike, the field growth at the trailing edge of the pulse being strongly saturated. The most interesting feature is that the spike can reach a duration well below the dephasing time $T_2 = 3.5$. As the pump power increases, the spike duration falls while its energy increases. It assumes a remarkably sym-

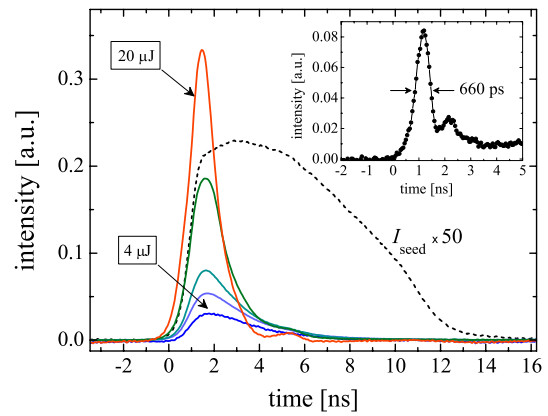


FIG. 2 (color online). Temporal structure of amplified Stokes pulses measured after propagation along 1.5 m of HC-PCF filled with H_2 at 3 bar for pump energies of 4, 8, 12, 16, and $20 \mu\text{J}$. The seed Stokes pulse is shown with a dashed line, magnified by a factor of 50. The inset shows a single shot measurement of the amplified Stokes pulse envelope at a pressure of 1.5 bar.

metric form, close to the $\text{sech}^2(x)$ shape in Eq. (1). This is not, as might be thought, the result of averaging over many shots, but is characteristic of every single shot—see the inset in Fig. 2. Above a certain level of pump energy, however, the temporal compression saturates to a minimum pulse duration of 1.3 ns—significantly shorter than T_2 . This cannot be attributed to the transient character of the Raman gain, because even shorter BRS pulses were observed when Stokes seed pulses with steeper pulse fronts were used.

The origin of this behavior can be understood by reference to Figs. 2 and 3(a). It is seen that, for pump energies in the range from 5 to $15 \mu\text{J}$, amplification of the spike is nearly uniform across its width, the peak of the spike remaining in approximately the same position. For pump energies $> 15 \mu\text{J}$, however, there is a noticeable shift of the peak to earlier times. In fact, the amplification is not uniform anymore, which translates into an apparent acceleration of the pulse, with a time advance that grows monotonically with the pump energy [Fig. 3(b)]. Interestingly, for large enough pump energy the shape of the output Stokes pulse becomes quite symmetric, remaining more or less unchanged as the pulse energy is further increased. We find that the duration of the output pulse is insensitive to linear loss, while strongly depending on the steepness of the leading edge of the seed pulse. In this connection, it is worth noting that the amplification factor for the Stokes pulse is at least an order of magnitude higher than the linear attenuation factor. This indicates that the observed stabilization of the Stokes pulse cannot be attributed to formation of a dissipative soliton [Eq. (1)], in which amplification is balanced by linear loss.

To describe the dynamics of pulse amplification in this regime, we consider pump and Stokes waves propagating, respectively, in the $+z$ and $-z$ directions, and represented by the fields

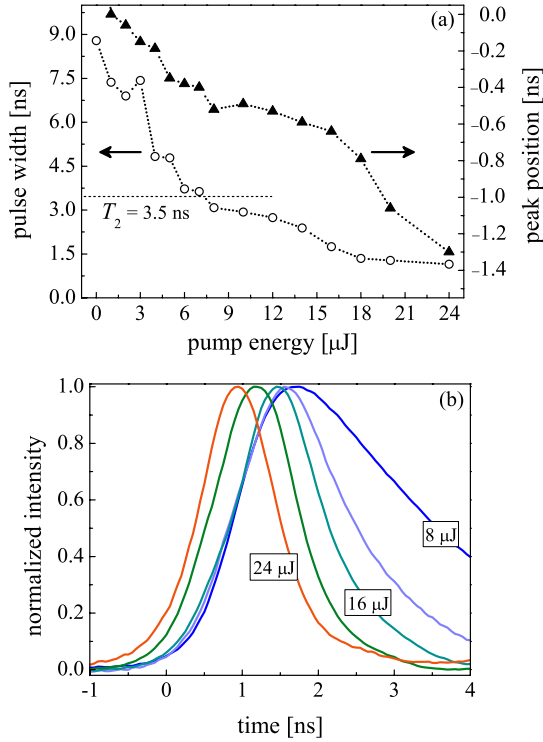


FIG. 3 (color online). (a) Duration and temporal position of the peak of the amplified Stokes pulses as a function of pump energy (HC-PCF is filled with hydrogen at 3 bar). (b) Experimental output Stokes pulse shapes (see Fig. 2) normalized to their peak intensity for increasing values of pump energy from right to left: 8, 12, 16, 20, 24 μJ .

$$E_{p,s}(z, t) = A_{p,s}(z, t) \exp(i\omega_{p,s}t \mp ik_{p,s}z) + \text{c.c.}$$

Here $A_{p,s}$ are the complex amplitudes and $\omega_{p,s}$ the carrier frequencies of the fields, which are two-photon resonant with the Raman transition, i.e., $\omega_p - \omega_s = \Omega$. The propagation constants of the guided modes in the fiber are $k_{p,s} = k(\omega_{p,s})$. Nonlinear propagation of the fields is described by the coupled wave equations:

$$\frac{\partial A_p}{\partial z} + \frac{1}{v_p} \frac{\partial A_p}{\partial t} = i \frac{\omega_p N r_{12}}{2\epsilon_0 c n_p} A_s \langle \rho_{12} \rangle - \frac{1}{2} \gamma_p A_p \quad (2a)$$

$$-\frac{\partial A_s}{\partial z} + \frac{1}{v_s} \frac{\partial A_s}{\partial t} = i \frac{\omega_s N r_{12}}{2\epsilon_0 c n_s} A_p \langle \rho_{12}^* \rangle - \frac{1}{2} \gamma_s A_s, \quad (2b)$$

where $n_{p,s}$, $v_{p,s}$ and $\gamma_{p,s}$ are the phase indices, group velocities and the linear attenuation coefficients of the two fields, respectively, and N is the number density of gas molecules in the hollow core. The two-photon matrix element $r_{12} = \hbar^{-1} \sum_i \mu_{1i} \mu_{i2} [(\omega_{i2} - \omega_s)^{-1} + (\omega_{i1} - \omega_p)^{-1}]$ (where μ_{mn} are the matrix elements of the dipole moment operator) characterizes Raman coupling of the molecules to the laser fields. The dynamics of the Raman transition, driven by pump and Stokes fields, are described by the density matrix elements ρ_{ij} ($i, j = 1, 2$):

$$\frac{\partial \rho_{12}}{\partial t} = -i\Delta\Omega \rho_{12} + i \frac{r_{12}}{4\hbar} A_p A_s^* n - \frac{\rho_{12}}{T_2} \quad (3a)$$

$$\frac{\partial n}{\partial t} = \frac{r_{12}}{\hbar} \text{Im}(A_p A_s^* \rho_{12}^*) - \frac{(n - n_0)}{T_1}, \quad (3b)$$

where the off-diagonal element ρ_{12} is the Raman coherence, $n = \rho_{11} - \rho_{22}$ is the population difference between the lower and upper levels, normalized to the total number of the gas molecules and n_0 is the equilibrium value of population in the absence of laser fields. Doppler broadening of the molecular frequency $\Delta\Omega = \Omega - (\omega_p - \omega_s)$ from the Raman resonance causes the two fields to form an inhomogeneous line shape described by the normalized function $g(\Delta\Omega)$, where $\int g(\Delta\Omega) d\Delta\Omega = 1$. The macroscopic medium response [i.e., the nonlinear source terms on the right-hand side of Eq. (2)] is calculated from $\langle \rho_{12} \rangle$ —the Raman coherence averaged over $g(\Delta\Omega)$. The modeling shows that the evolution of the Stokes pulse separates into two phases (Fig. 4). In the initial stages of the interaction, amplification is most effective at the leading edge of the seed pulse, causing the pulse front to steepen and the effective pulse duration to fall. This temporal narrowing does not stop even when the pulse duration is shorter than T_2 . This is explained by the fact that when the Stokes pulse becomes sufficiently strong (Fig. 4, $t = 2$ ns), the counter-

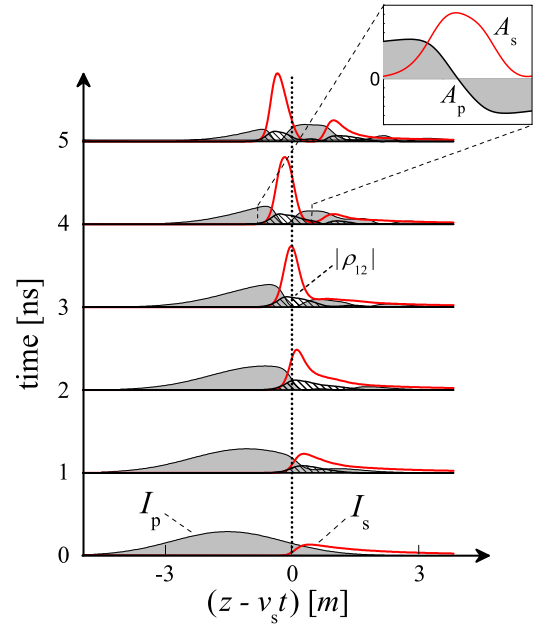


FIG. 4 (color online). The intensity envelopes of the pump (shaded in gray) and Stokes (red line) pulses shown at different times in a reference frame moving at the Stokes velocity v_s . Temporal compression of the Stokes pulse ($t < 3$ ns) is followed by the formation of a quasisoliton pulse traveling faster than the velocity of light v_s (the vertical dashed line shows the position of Stokes light moving at exactly v_s). The inset shows the amplitudes of the pump and the quasisoliton pulse. Also shown is the long-lived Raman coherence at Doppler line center (slanted line fill).

propagating pump wave is completely depleted before it reaches the trailing edge of the Stokes pulse. As a result, growth of the Stokes field [which is proportional to the source term in the right-hand side of Eq. (3a)] saturates at the trailing edge. One might expect, therefore, that a further increase in Stokes intensity would lead to even shorter pulse durations. The computer simulations show, however, that the Stokes pulse stabilizes to a near symmetric solitary structure whose envelope propagates faster than the velocity of light (Fig. 4, $t > 2$ ns). This reshaping effect does not contravene relativity, but is instead the consequence of pulse reshaping through (a) nonlinear amplification at the leading edge and (b) nonlinear absorption at the trailing edge by energy back conversion to the pump frequency. It is the long-lived Raman coherence which is responsible for this reshaping process. We also note some similarity between this process and the propagation of coherent 2π pulses in laser amplifiers [11]. The formation of a pulse moving faster than the speed of light is caused by the presence of the long exponential leading edge of the seed pulse. After propagation over a certain amplification length, the pulse peak finally approaches the “earliest point” on the leading edge of the seed pulse. From this moment on, the pulse would be further amplified, its duration falling as it approaches the asymptotic form described by Eq. (1). Under our experimental conditions, however, the pulse peak reaches the end of the amplifying medium before approaching the “earliest point”.

Some basic properties of the BSRS equations can be extracted by considering solutions of Eqs. (2) and (3) in the form of an invariant pulse profile that depends on the variable $\tau = t - z/v$ where $v > v_s$. We assume that this Stokes pulse is amplified by an infinitely long pump wave with constant amplitude A_0 . Neglecting inhomogeneous line broadening and linear loss in the system, after some manipulation of Eqs. (2) and (3), we find that the coherence is purely imaginary, $\rho_{12} = i\rho$, obeying the differential equation:

$$\frac{\partial^2 \Psi}{\partial \tau^2} + \frac{1}{T_2} \frac{\partial \Psi}{\partial \tau} = \beta^2 \sin \Psi \quad (4)$$

where we have introduced the function

$$\Psi(\tau) = \alpha \int_{-\infty}^{\tau} \rho(\tau') d\tau' \quad (5)$$

and the parameter $\alpha = (r_{12} N_0 / \epsilon_0) [\omega_p \omega_s / (v_s^{-2} - v^{-2})]^{1/2}$ with $N_0 = n_0 N$. The parameter β in Eq. (5) is related to α through $(\alpha/\beta)^2 = 2(N_0/N_p)(v_p n_p/c)$, where $N_p = 2\epsilon_0 n_p^2 A_0^2 / \hbar \omega_p$ is the initial photon density in the pump field. We seek solutions of Eq. (4) with initial conditions $\Psi(-\infty) = \Psi'(-\infty) = 0$. The behavior of such solutions depends on the dimensionless parameter βT_2 and describes nonlinear oscillations asymptotically approaching the equilibrium value $\Psi(+\infty) = \pi$. However, in the limit of long dephasing times, $\beta T_2 \gg 1$, the relaxation term in Eq. (4) can be neglected, and Eq. (5) has the 2π pulse

solution $\Psi(\tau) = 4 \arctan[\exp(\tau/\tau_0)]$ associated with a solitary pulse of the coupled Stokes and pump fields:

$$A_s(\tau) = A_0 [\omega_s(v + v_s) / \omega_p(v - v_s)]^{1/2} \text{sech}(\tau/\tau_0) \quad (6a)$$

$$A_p(\tau) = -A_0 \tanh(\tau/\tau_0). \quad (6b)$$

The characteristic duration τ_0 is given by the expression:

$$\frac{1}{\tau_0^2} = \frac{\omega_s N_0 r_{12}^2}{8\epsilon_0 c \hbar (v_s^{-1} - v^{-1})} A_0^2. \quad (7)$$

It follows from Eq. (6) that, at the point where the Stokes field reaches its maximum, the pump field goes through a zero, in direct agreement with the results of the numerical simulations (see inset in Fig. 4). We also note that, unlike dissipative solitons in amplifying media [2,12,16], the pulse duration in Eqs. (5)–(7) is not fixed, i.e., it is a free parameter. Therefore, a seed Stokes pulse having an exponential leading edge (with characteristic time τ_0) will evolve towards a sech profile of the same duration traveling at a velocity $v(\tau_0)$ determined by the dispersion relation (7). The velocity of such a solitary Stokes pulse increases roughly linearly with the pump intensity. These considerations qualitatively explain the experimental observations (Figs. 2 and 3) and support the numerically-modeled pulse dynamics presented in Fig. 4. Finally, we note that by minimizing loss in a specially engineered fiber and optimizing the experimental configuration, pulse compression factors much greater than 20 should be possible.

*www.pcfiber.com

†http://laser.cheng.cam.ac.uk

- [1] M. Maier *et al.*, Phys. Rev. Lett. **17**, 1275 (1966).
- [2] M. Maier and W. Kaiser, Phys. Rev. **177**, 580 (1969).
- [3] J.R. Murray *et al.*, IEEE J. Quantum Electron. **15**, 342 (1979).
- [4] R.L. Carman *et al.*, Phys. Rev. A **2**, 60 (1970).
- [5] M.D. Duncan *et al.*, J. Opt. Soc. Am. B **5**, 37 (1988).
- [6] I.G. Koprnikov *et al.*, J. Opt. Soc. Am. B **16**, 267 (1999).
- [7] Z. Ye *et al.*, Chin. Opt. Lett. **1**, 406 (2003); H. Nishioka *et al.*, IEEE J. Quantum Electron. **29**, 2251 (1993).
- [8] P. St. J. Russell, J. Lightwave Technol. **24**, 4729 (2006).
- [9] F. Benabid *et al.*, Science **298**, 399 (2002).
- [10] F. Benabid *et al.*, Phys. Rev. Lett. **93**, 123903 (2004).
- [11] P.G. Kryukov and V.S. Letokhov, Sov. Phys. Usp. **12**, 641 (1970); A.N. Oraevsky, Sov. Phys. Usp. **41**, 1199 (1998).
- [12] R. Bonifacio *et al.*, Phys. Rev. A **12**, 2568 (1975); J.D. Harvey *et al.*, Phys. Rev. A **40**, 4789 (1989).
- [13] G. Herzberg, *Molecular Spectra and Molecular Structure* (Krieger Publ., Florida, 1989), Vol. I.
- [14] J.R. Murray and A. Javan, J. Mol. Spectrosc. **42**, 1 (1972); A. Owyong, Opt. Lett. **2**, 91 (1978).
- [15] A.Z. Grasyuk *et al.*, Sov. J. Quantum Electron. **12**, 14 (1982).
- [16] E. Picholle *et al.*, Phys. Rev. Lett. **66**, 1454 (1991).